

## Mild Steel Corrosion Inhibition by Benzotriazole in 0.5M Sulfuric Acid Solution on Rough and Smooth Surfaces

M. Amini<sup>1</sup>, M. Aliofkhazraei<sup>1,\*</sup>, A.H. Navidi Kashani<sup>2</sup>, A. Sabour Rouhaghdam<sup>1</sup>

<sup>1</sup> Department of Materials Engineering, Tarbiat Modares University, P.O. Box: 14115-143, Tehran, Iran

<sup>2</sup> School of Metallurgy and Materials Engineering, College of Engineering, University of Tehran.

\*E-mail: [maliofkh@gmail.com](mailto:maliofkh@gmail.com), [khazraei@modares.ac.ir](mailto:khazraei@modares.ac.ir)

*Received:* 19 April 2017 / *Accepted:* 22 July 2017 / *Published:* 13 August 2017

---

The corrosion inhibition of benzotriazole in 0.5 M sulfuric acid solution is evaluated on the mild steel specimens with two amounts of surface roughness. Benzotriazole adsorption on mild steel surface followed Langmuir isotherm. The corrosion inhibitor has generally physisorption on both surfaces. The results obtained by the different experimental methods showed good agreement with each other. Results of FTIR test showed a peak related to C-H bond for both surfaces as a proof of the presence of benzotriazole on the steel's surface which its intensity was higher for rough surface because of more adsorption of corrosion inhibitor on the surface.

---

**Keywords:** Benzotriazole, Corrosion, Mild Steel, Roughness, Sulfuric Acid.

### 1. INTRODUCTION

Steel components are widely used under different conditions in chemical and associated industries in alkaline, acidic and saline environments [1]. Generally acidic solutions are used to remove rust and undesirable materials in industrial operations [2]. Chloride, sulfate and nitrate ions are aggressive ions in the aqueous environments and usually accelerate corrosion [1]. The corrosive acidic environments are widely used for industrial purposes and the corrosion inhibitors are usually used to control the dissolution of the metal. Many known acidic organic corrosion inhibitors are compounds including nitrogen, sulfur and oxygen atoms. It is proved that many N-heterocyclic's compounds are effective corrosion inhibitor of metals and alloys in the aqueous environments [3]. Corrosion inhibitor of steel's corrosion in acidic environments is studied by some of the organic compounds containing nitrogen [4, 5]. These compounds can be adsorbed onto the surface of metals, block the surface-active areas and thus reduce corrosion [5]. This phenomenon is affected by the metal's nature, surface charge,

type of aggressive electrolyte and chemical structure [1]. Generally the nitrate compounds are effective as anodic corrosion inhibitors for mild steel; however there are limitations in using them, including environmental restrictions due to their toxic effects, mechanisms of corrosion inhibition, the tendency to mechanical losses, the risky effects when they are not used in sufficient quantities, and the high cost of these types of compounds. One of the widely triazole-type nitrogen containing corrosion inhibitors is benzotriazole (BTA). It is an effective corrosion inhibitor for copper and stainless steel in the acidic environments [6]. This corrosion inhibitor is an organic compound and contains benzene and triazole rings which are organic heterocyclic compounds.

Evgeny et al. [7] studied the effect of surface roughness and flow type on the corrosion behavior of mild steel in 4 M hydrochloric acid solution in the presence of corrosion inhibitor. They indicated that immersion in a solution containing corrosion inhibitor resulted in slight decrease average surface roughness for the rougher surfaces and also corrosion increased by increasing the surface roughness. Saad Ghareba et al. [8] studied the corrosion inhibition of carbon steel, immersion time, pH and surface roughness and the results indicated that the 11-aminoundecanoic acid has similar effects on surfaces with different roughness levels, indicating the good effect of this corrosion inhibitor.

Gomo et al. [9] studied the corrosion inhibitor effect of BTA on 1 M sulfuric acid solution on mild steel which indicates that the corrosion potential and polarization resistance are increased by increasing the corrosion inhibitor concentration while the critical current and corrosion rate are being reduced. The researchers have proved that the corrosion rate depends on the corrosion inhibitor concentration, chloride ion and the scan rate of polarization. The highest corrosion inhibition efficiency is obtained at  $9 \times 10^{-3}$  M and it was 98.5%. It was found that corrosion current density increases with scan rate.

Various researchers have conducted studies on the corrosion inhibitor effect of BTA derivatives on steel in different solutions [10-12]. According to Selvi et al. [1], the efficiency of  $448 \times 10^{-4}$  M BTA for mild steel which is prepared by the sandpaper #1200 in 0.5 M  $H_2SO_4$  solution reached 70%. It also reached 97% by replacing the 1-hydroxy methyl benzotriazole as corrosion inhibitor with a lower amount. Researchers have studied the effects of surface conditions such as microstructure [13], surface morphology [14] and fine grained surface [15] on the adsorption of corrosion inhibitor on the metal's surface. The aim of this study is changing the surface roughness to reach higher corrosion inhibitor efficiency for steel in 0.5 M sulfuric acid solution. It is expected that the corrosion rate is reduced by roughening the surface in the presence of corrosion inhibitor and the efficiency of the corrosion inhibitor and thus the adsorption energy of the corrosion inhibitor were increased on rough surface.

Sour acids are widely used in the industry for acid washing and degreasing. Moreover the acids are widely used in numerous manufacturing processes in various industries. The metals that used for operations such as painting, galvanizing, cold drawing, and electroplating, should have clean surfaces and been free of any salts and oxides. Undesirable materials should be removed from metal's surfaces, so the metal should be immersed in an acidic solution .e.g. hydrochloric acid, sulfuric acid, nitric acid, oxalic acid and so on. Acidic solutions usually attack the metal's surface; so to reduce the corrosion, the corrosion inhibitor is added to the sour acid solution [3].

The aim of this study is to evaluate the effect of rough surface on corrosion of mild steel in 0.5 M H<sub>2</sub>SO<sub>4</sub> solution. Thus by comparison with smooth steel, the impact of roughness parameter and corrosion inhibitor concentration on the adsorption of BTA corrosion inhibitor is studied by potentiodynamic polarization, electrochemical impedance spectroscopy (EIS) and weight loss measurement.

## 2. EXPERIMENTAL PROCEDURE

### 2.1. Material preparation

Specimens of mild steel with dimensions of 0.2×3×2 cm<sup>3</sup> were used. The specimen's surfaces were prepared in two forms. A group of specimens was abraded by the sandpapers #800, #1000, #1500, #2000, #2500 and #3000, while the other group was being prepared by just sandpaper #320. The R<sub>a</sub> roughness parameter (measured by Talor-Habson, Surtronic-25 surface profilometer) for the first group was 0.12±0.01 μm and R<sub>10</sub> parameter was 0.156%, while the R<sub>a</sub> for the second group was 4.3±0.01 μm and R<sub>10</sub> was 3.28%. All specimens were washed by alcohol and deionized water (18 MΩ) after preparation. Specimen preparation was performed according to ASTM G1 standard [16]. Solutions were prepared using analytically pure H<sub>2</sub>SO<sub>4</sub> with 0.5 M concentration. In order to analyze the corrosion inhibition effect, BTA (Merck) was added to solutions with the concentrations of 0.00025, 0.005, 0.0075 and 0.01 M. All tests were done three times for all samples to ensure the repeatability of results.

### 2.2. Weight loss measurement

The weight loss measurement was conducted according to ASTM G31 standard [17]. Steel specimens were weighed before and after immersion in corrosive solution by high-precision microbalance (AND-GR202) with the precision of ±50 μgr. They were exposed to 100 ml of 0.5 M H<sub>2</sub>SO<sub>4</sub> solution with different concentrations of benzotriazole. Five solutions were prepared containing 0, 0.0025, 0.005, 0.0075 and 0.01 M BTA and the immersion in these solutions took 96 hours. The pH of the solutions was 0.27 and addition of BTA did not change pH considerably.

After immersion, the specimens were removed from the solution and after being rinsed with deionized water and dried, they were weighted again. Weight loss measurements were done at a temperature of 25±2°C. The corrosion rate (*v*) was calculated using the equation (1):

$$v = \frac{W}{St} \quad (1)$$

Where, W is the average weight loss of steel specimen, S is the surface area of the steel specimen, and t is the duration of immersion. Using the calculated corrosion rate, corrosion inhibition efficiency (IE) was calculated by using the equation (2):

$$IE \% = \frac{v_0 - v}{v_0} \times 100 \quad (2)$$

Where,  $v$  and  $v^\circ$  are the corrosion rate values with and without addition of the BTA corrosion inhibitor [18].

### 2.3. Potentiodynamic polarization

Potentiodynamic polarization tests are done based on ASTM G5 [19] by EG&G potentiostat-galvanostat (model 273A). All tests are done at  $25 \pm 0.5^\circ\text{C}$  by three-electrode set up using a saturated calomel electrode (SCE) as reference electrode, platinum sheet as auxiliary electrode and steel specimen as the working electrode. Before running the test, the system was given 30 minutes to reach stabilized open circuit potential (OCP). The potential scanned from  $-250$  mV vs. OCP to  $+250$  mV vs. OCP with the scan rate of  $0.5$  mV/s. Corrosion rates are obtained by tafel linear extrapolation. The required data are obtained by powersuite software and the efficiency is calculated according to the equation (3):

$$IE = \frac{i^\circ - i}{i^\circ} \times 100 \quad (3)$$

$i^\circ$  and  $i$  are the corrosion rates of the specimen with and without the corrosion inhibitor and  $IE$  is the corrosion inhibition efficiency.

### 2.4. EIS tests

EIS was conducted based on ASTM G106 standard [20] by EG&G potentiostat-galvanostat (model 273A equipped with frequency response analyzer system). Mild steel samples with the contact surface area of  $0.785$  cm<sup>2</sup> were used as the working electrode. During the EIS test, the frequency range varied between  $0.01$  Hz to  $100$  kHz and the alternating voltage amplitude was  $10$  mV. Zview2 software was used to analyze the impedance data and modeling with equivalent electrical circuits.

### 2.5. Surface analysis

After immersion of mild steel specimens, the surface morphologies of specimens were analyzed by scanning electron microscope (Philips XL-30) with  $20$  kV bias voltage under secondary electron mode. Fourier-transform infrared Spectroscopy (FTIR) was also done on specimens by a spectrophotometer within the range of  $4000$ - $400$  cm<sup>-1</sup>.

## 3. RESULTS AND DISCUSSION

### 3.1. Weight loss measurement

Table 1 presents the calculated values of  $v$  and  $IE\%$  at different concentrations of corrosion inhibitor. The results showed that  $IE\%$  was increased by increasing the corrosion inhibitor concentration while the corrosion of the rough specimen in the solution without corrosion inhibitor is

higher than the smooth specimen. With increasing concentration of the corrosion inhibitor, the efficiency was increased and reached 53% for the smooth specimen and 75% for the rough specimen and it is similar to other report [1].

**Table 1.** corrosion rate values obtained by the weight loss measurement for mild steel with smooth and rough surfaces in 0.5 M H<sub>2</sub>SO<sub>4</sub> solution and different concentrations of BTA inhibitor.

BTA concentration (m.L <sup>-1</sup> )	Corrosion rate (μgr.cm <sup>-2</sup> h <sup>-1</sup> )	IE <sub>w</sub> (%)
Smooth steel		
Blank	476	
0.0025	264	44
0.005	175	47
0.0075	248	48
0.01	223	53
Rough steel		
Blank	687	
0.0025	236	65
0.005	201	70
0.0075	157	74
0.01	172	75

3.2. Potentiodynamic polarization measurements

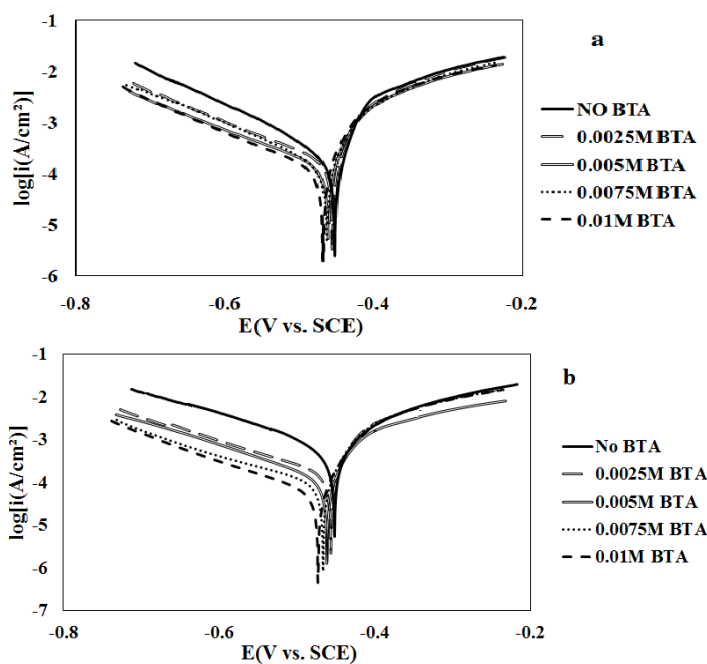


**Figure 1.** Polarization curves of mild steel with (a) smooth surface and with (b) rough surface in 0.5 M H<sub>2</sub>SO<sub>4</sub> solution with the scan rate of 0.5 mV/s within the potential range of -250 to 250 compared to OCP. The potentials are measured versus the Calomel reference electrode in 25 °C.

Figure 1 presents the potentiodynamic polarization curves of steel with smooth (Fig.1a) and rough (Fig.1b) surface in 0.5 M H<sub>2</sub>SO<sub>4</sub> solution containing different concentrations of BTA. The tests were done after exposure to solution for 30 minutes. In the solutions without corrosion inhibitor, in the anodic branch, steel dissolution and in the cathodic branch, hydrogen evolution reaction was occurred. It is obvious that in the presence of corrosion inhibitor, the anodic and cathodic curves are displaced and the level of this displacement depends on the concentration of the corrosion inhibitor. Polarization parameters such as corrosion potential and corrosion current density were obtained by linear tafel extrapolation from the curves in Figure 1, and were summarized in Table 2.

**Table 2.** Changes in the corrosion inhibitor efficiency (IE), the corrosion potential ( $E_{\text{corr}}$ ) and corrosion current density ( $i_{\text{corr}}$ ) in the absence and presence of various concentrations of Benzotriazole as an corrosion inhibitor in 0.5 M H<sub>2</sub>SO<sub>4</sub> solution for mild steel specimens with smooth and rough surface through linear extrapolation of tafel zone.

BTA concentration(mol L <sup>-1</sup> )	$E_{\text{corr}}$ (mV vs. SCE)	$i_{\text{corr}}$ ( $\mu\text{A}\cdot\text{cm}^{-2}$ )	IE <sub>t</sub> %
Smooth steel			
Blank	-454	70.8	
0.0025	-455	42	40
0.005	-457	37	47.7
0.0075	-460	30	57
0.01	-462	28.4	59
Rough steel			
Blank	-449	101	
0.0025	-458	40	60
0.005	-462	32	68
0.0075	-467	22.6	77
0.01	-475	20.18	80

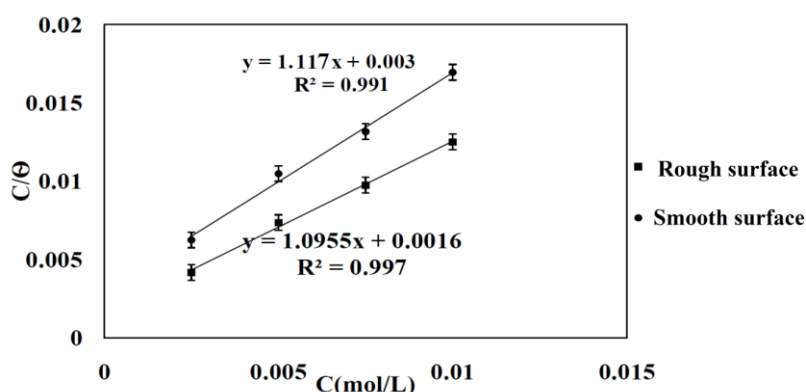
With increasing the concentration of corrosion inhibitor, little changes were occurred and the corrosion current density was reduced. Similar changes were also observed elsewhere [1]. Adding benzotriazole prevents the acid attack to the steel's surface. Comparing the anodic and cathodic branches of the curves indicates that by increasing the corrosion inhibitor concentration, the current density in both anodic and cathodic branches were reduced which indicates that the corrosion inhibitor worked as mixed type on mild steel in this solution. The presence of corrosion inhibitor in the corrosive solution caused an increase in the overvoltage of anodic and cathodic branches and reduced the corrosion current density. These changes are increased by increasing the concentration of corrosion inhibitor and this behavior indicates the corrosion inhibitor adsorption on the metal's surface and protective effect on the transfer of electrical charges and ions in the anodic and cathodic reactions [21].

Table 2 also presents the efficiency calculated based on equation (3). It is clear that these values have been increased with increasing concentrations of corrosion inhibitors for both surfaces which indicate achieving higher amounts of surface coverage. By increasing the concentration of corrosion inhibitor from 0.0075 M to 0.01 M, no change was observed in the efficiency. The efficiency levels for the rough surface presented higher values which indicate higher surface coverage for the rough surface. Corrosion inhibitor efficiencies that were obtained by polarization were summarized in Table 2. The results showed a good match with the efficiency obtained by the weight loss measurement. In both of them, the highest efficiency was associated with the rough specimen and the concentration of 0.01 mol.L<sup>-1</sup> of the corrosion inhibitor.

For the smooth specimen, corrosion current density was 70.8  $\mu A/cm^2$  in solution without corrosion inhibitor. By addition 0.01 M of corrosion inhibitor, the corrosion current density was reached to 28.4  $\mu A/cm^2$  and thus the efficiency was reached to 59%. In the case of rough surface, in the absence of corrosion inhibitor, corrosion current density is higher due to the existence of active areas and the corrosion current density is 101  $\mu A/cm^2$  and thus by addition of corrosion inhibitor with the concentration of 0.01 M, it was reached to 20.18  $\mu A/cm^2$  with the efficiency of 80%. Further increase of corrosion inhibition efficiency at higher concentrations on the rough surface indicates higher adsorption of the corrosion inhibitor molecules on the metal's surface and thus indicates higher surface coverage. This corrosion inhibitor acts as an adsorbent corrosion inhibitor. According to Table 2, benzotriazole for the rough specimen in 0.5 M H<sub>2</sub>SO<sub>4</sub> is a more effective corrosion inhibitor than the smooth surface.

### 3.3. Adsorption isotherm

Adsorption of BTA on steel's surfaces never reaches equilibrium, but it tends to reach the stable state. When the corrosion rate is effectively low, the steady state adsorption tends to achieve a quasi-equilibrium state and in this case, it is necessary to consider the quasi-equilibrium adsorption by thermodynamic calculations considering appropriate equilibrium isotherm. The adsorption isotherm could provide basic information about the reaction between the metal's surface and corrosion inhibitor [22].



**Figure 2.** Langmuir adsorption isotherm curve obtained from the covering number of the surface obtained by polarization curves for smooth and rough specimens in H<sub>2</sub>SO<sub>4</sub> 0.5 M solution.

Corrosion inhibitor efficiency depends on the type and number of active sites on the metal's surface, charge density, size of the corrosion inhibitor molecules, reaction between metal and corrosion inhibitor and complex layer formation. To obtain the adsorption isotherm, the coverage of the surface ( $\Theta$ ) at various concentrations of BTA according to polarization curves was obtained according to equation (4):

$$\theta = \frac{i^{\circ} - i}{i^{\circ}} \quad (4)$$

Where  $i^{\circ}$  and  $i$  are the corrosion current density in absence and presence of corrosion inhibitor, respectively. The relationship between  $\Theta$  and corrosion inhibitor concentration with corrosive solution is presented through the following equation by Langmuir adsorption isotherm [21, 23, 24]:

$$\frac{C_{inh}}{\theta} = \frac{1}{K_{ads}} + C \quad (5)$$

Where,  $C$  is the corrosion inhibitor concentration and  $K_{ads}$  is the equilibrium adsorption constant. The relationship between  $C_{inh}/\Theta$  and  $C_{inh}$  is presented in Figure 2. According to this figure, linear relationship between  $C_{inh}/\Theta$  and  $C_{inh}$  can be seen. This behavior indicates that benzotriazole adsorption on steel's surface obeys Langmuir isotherm adsorption. This isotherm supposes that the adsorbed molecules only form single molecular layer and the adsorbed molecules form a homogeneous and uniform layer without interacting with each other [21, 25].

There is a good agreement between the experimental data and langmuir adsorption isotherm ( $R^2=0.9933$  for smooth specimen and  $R^2= 0.997$  for the rough specimen while the slope of the curves is close to 1) [26]. The value of  $K_{ads}$  for the smooth and rough specimens is 333 and 625 mol/L, respectively. The amount of adsorption energy ( $\Delta G_{ads}$ ) for the corrosion inhibitor molecules was obtained using the following equation [13]:

$$K_{ads} = \frac{1}{55.5} \exp\left(\frac{-\Delta G_{ads}}{RT}\right) \quad (6)$$

The value of free energy of the adsorption is -26 kJ/mol for the rough surface and -24 kJ/mol for the smooth surface. Negative values of  $\Delta G_{ads}$  are equal with -20 kJ/mol or the lower values are associated with the electrostatic interaction between the charged molecules and charged metals (physisorption). The ones that are about -40 kJ/mol or higher are subject to share the charges or transfer from organic molecules to the metal's surface to form a coordination bond (chemisorption) [27]. Released energy values between these two numbers are associated with complex corrosion inhibitor adsorption and the calculated  $\Delta G_{ads}$  presented a value in this range which is closer to -20kJ/mol, so the adsorption of corrosion inhibitor is mixed-type adsorption closer to physisorption [28]. In physisorption, the electrostatic interaction happens between the charged molecules and the charged surface of the metal. More negative value for  $\Delta G_{ads}$  represents the spontaneous, corrosion inhibitor adsorption on the metal's surface [29-31]. By reducing the roughness, the released energy amount becomes more positive which indicates the reduced tendency to adsorb corrosion inhibitor on the metal's surface. By reducing roughness, the value of free energy tends to less negative values and it indicates lower tendency on adsorption of corrosion inhibitor on metal's surface. In other word, with decreasing the roughness, corrosion inhibitor efficiency was decreased [28].

Corrosion inhibition performance of the organic molecules that include sulfur, nitrogen or oxygen atoms is known by forming the coordination bonds between metal and the lone pair of electrons. Similarly, benzotriazole adsorption on the metal's surface is done directly by the electron

donor and receptor between the corrosion inhibitor P-electrons and the vacancies in orbital d of the surface atoms or the adsorbed sulfate ions [32-36].

### 3.4. EIS study

For more information about the corrosion inhibitor performance and the authentication of the obtained data of the potentiodynamic polarization tests, the electrochemical impedance spectroscopy is done on steel specimens. EIS is a powerful method to study the corrosion mechanism [37]. Relating the impedance curve to an equivalent electrical circuit, leads to the confirmation of a mechanism for the system. Such relation leads to the calculation of the numeric value associated with the physical or chemical properties [38]. As it has been reported in many references, steel will be protected in the presence of BTA corrosion inhibitor in acidic solutions with two mechanisms. This corrosion inhibitor either protects the surface by adsorption on sample or prevention of aggressive ions or forms a complex layer by reaction with the substrate's surface, including the corrosion inhibitor molecules and surface oxides. Impedance studies are conducted in two parts; first at the beginning of immersion and second by passing the time.

First, the corrosion inhibition effect at the beginning of the immersion is studied to analyze the effect of surface roughness and determining of optimum concentration. Accordingly, the EIS measurements of rough and smooth specimens were conducted in the absence and presence of different concentrations of corrosion inhibitor.

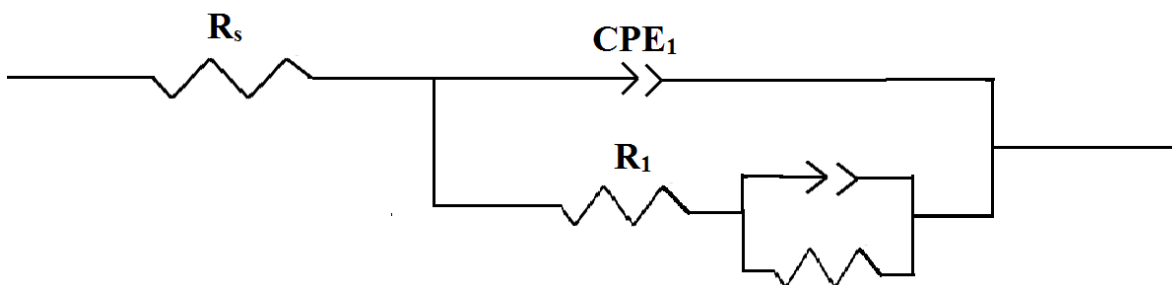


**Figure 3.** Equivalent circuit used to fit the impedance data of steel in 0.5 M H<sub>2</sub>SO<sub>4</sub> solution at the beginning of immersion in the absence and presence of various concentrations of BTA inhibitor

The equivalent electrical circuit, shown in Figure 3, is used to fit the EIS data and extract information. In the equivalent circuit, a resistance and time constant are considered. In the equivalent electrical circuit, R<sub>s</sub> indicates the solution resistance, R<sub>1</sub> represents the electrical double layer (EDL) resistance and CPE<sub>1</sub> represents the constant phase element of the EDL. As it can be observed in this study, the constant phase element is used instead of pure capacitor, due to the heterogeneous factor of the surface [39, 40]. In this regard the constant phase element impedance is defined as follows:

$$Z_{CPE} = \frac{1}{T(j\omega)^n} \tag{7}$$

Where, T is the admittance constant, j is imaginary unit, ω is angular frequency and n is the CPE experimental power that usually varies among 0 and 1. The values of 0 and 1 for n indicate pure

resistance and capacitance, respectively;  $n$  has a direct correlation with surface roughness and its proximity to 1 indicates higher smoothness and proximity to 0 indicates more roughness.

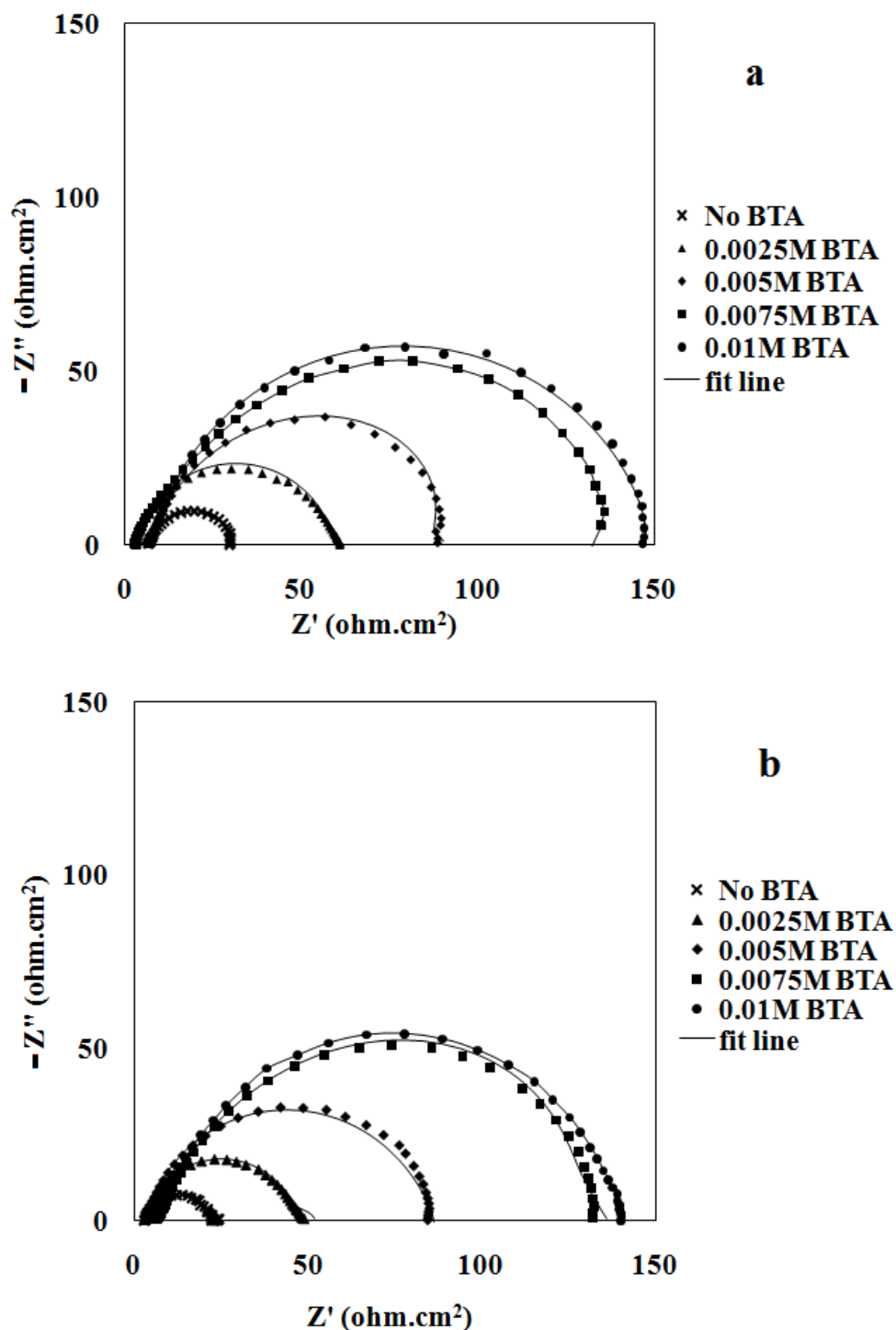


**Figure 4.** Nyquist diagram of the mild steel specimens in 0.5 M H<sub>2</sub>SO<sub>4</sub> solution with different concentrations of corrosion inhibitor as soon as immersion of the a) smooth and b) rough specimens in solution.

Figure 4 shows nyquist diagram for rough and smooth specimens at different concentrations of BTA. Nyquist curves did not show ideal capacitive semicircle. An imperfect semicircles can be associated with the frequency dispersion achieved as a result of electrode surface roughness and heterogeneity [41, 42]. Figure 4 shows that the semicircles size increased with increasing corrosion inhibitor's concentration in the corrosive solution. These two figures are related to the nyquist diagrams of samples as soon as their immersion and the diagrams related to the rough surface present higher resistance. Since increasing this radius is equal with increasing the polarization resistance, the corrosion resistance is increased by the concentration of the corrosion inhibitor in the solution for both rough and smooth surfaces. This behavior was mentioned in most references for smooth surfaces. By increasing the corrosion inhibitor concentration, the corrosion inhibitor rate increases until it reaches a constant level.

According to Saad Ghareba et al. [8] and Feng et al. [12], the size of the semicircle represents improvement of the adsorbed corrosion inhibitor film structure and lower corrosion rate, which is consistent with results obtained in this section. Figure 4 suggests that by increasing the corrosion inhibitor concentration, the semicircle radius was increased and eventually semicircle radius is constant at high BTA concentrations, which is probably the maximum corrosion inhibition. This figure also suggests that at first, the semicircle radius or resistance has been lowered for the rough surface but at higher concentrations the resistance on rough and smooth surfaces is equal. This behavior indicates that the rough surface has a better performance at higher concentrations. In the case that there is no corrosion inhibitor in the solution, the cavities of rough surface are suitable for aggressive ions accumulation and intensify corrosion conditions. In general, it has high number of active sites and the conditions are dangerous for active surface. This causes the rough specimens resistance to be low in the solution without corrosion inhibitor. By increasing the concentration of the corrosion inhibitor, the resistance of both surfaces will be gradually equal, which indicates that the corrosion inhibitor could protect the surface; i.e. despite the seriousness of the initial conditions for rough surface, the conditions are compensated by increasing the corrosion inhibitor concentration even in high concentration of corrosion inhibitor, resistance of rough surface was increased. Noor et al. [43] reported that if the surface is rough, it is possible to apply the corrosion protection conditions as same as the smooth surface by increasing the concentration of corrosion inhibitor. As the curves for both specimens in Figure 4 suggest, the rough specimen with 0.01 M BTA has the highest semicircle diameter or the highest corrosion resistance, even more than the smooth specimens with the same condition. By increasing the surface roughness, the actual surface in contact with the corrosive solution will increase and such conditions are worse without corrosion inhibitor [44]. Presence of enough amount of corrosion inhibitor that could cover the surface completely, could improve the conditions. Considering more surface in rough sample, the possibility of adsorbing the corrosion inhibitor molecules increases [43].

Figure 5 presents bode and bode-phase curves for rough and smooth surfaces in different concentrations of BTA. As it can be observed in bode-phase curves, all curves have a peak which indicates that their behavior is single time constant. The equivalent electrical circuit also showed one time constant related to the EDL.

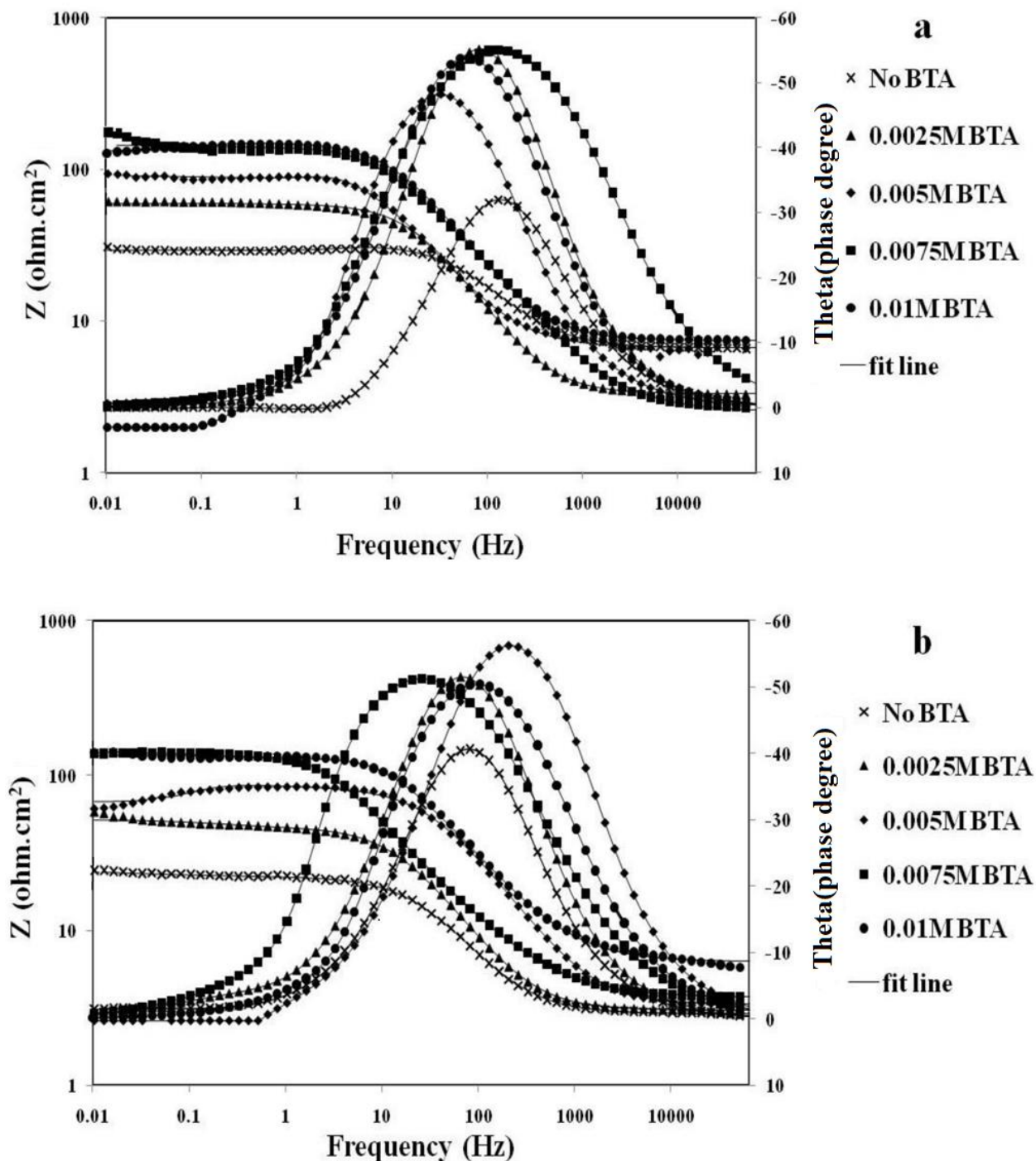


**Figure 5.** Bode and Bode-phase diagrams of the steel specimens with a) smooth and b) rough surfaces as soon as immersion in 0.5 M H<sub>2</sub>SO<sub>4</sub> solution with different concentrations of corrosion inhibitor.

As the curves suggest, by increasing the corrosion inhibitor concentration, the phase angle values tend to negative values which indicate the capacitive behavior and higher resistance to the passing of water and ions. This behavior is observed in both smooth and rough surfaces but it can be seen better at higher concentrations. By increasing the BTA concentration on both rough and smooth

surfaces, the total resistance or the resistance at the lowest frequency, increases which confirms the results of polarization (fig. 5).

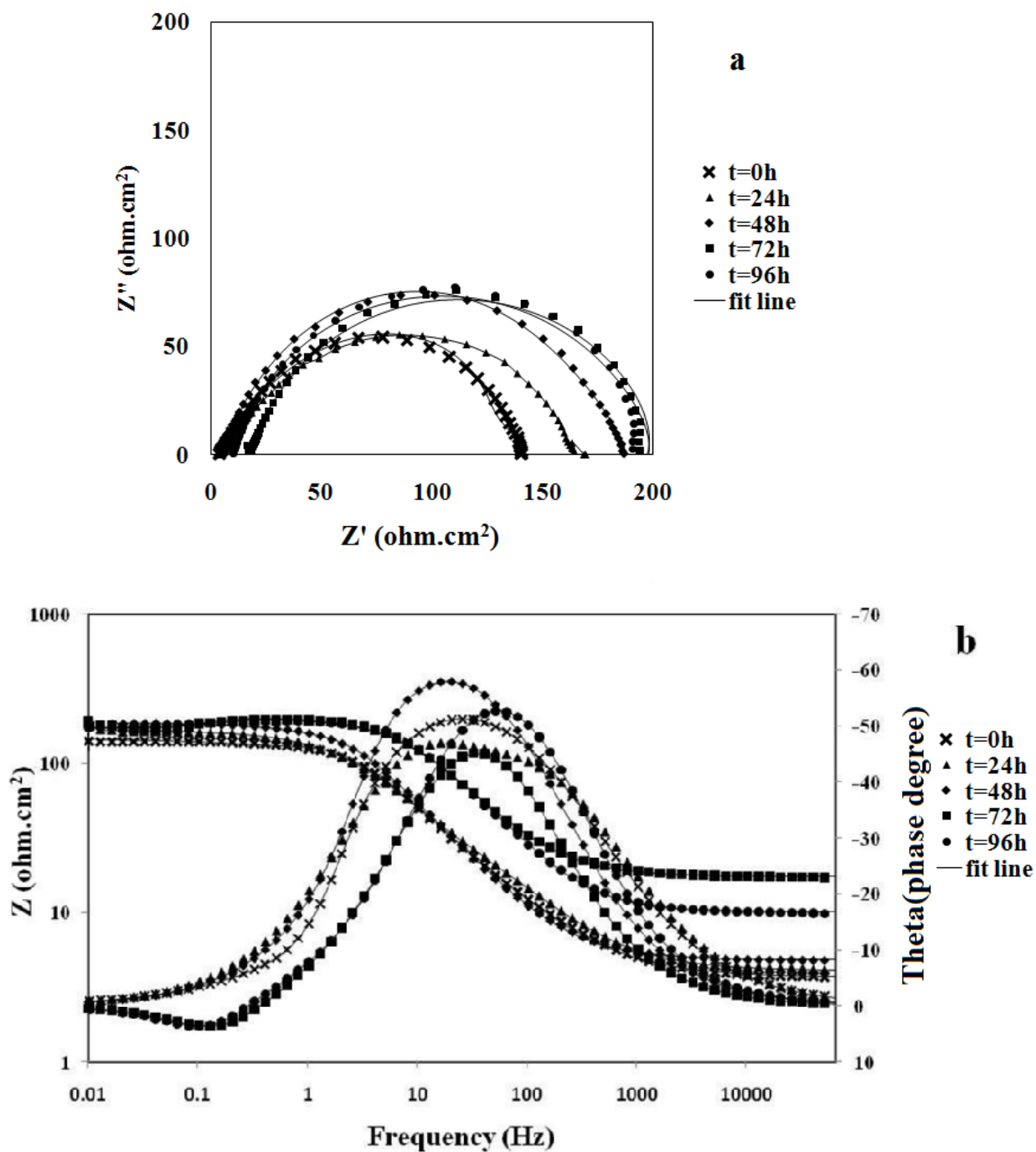


**Figure 6.** a) Nyquist diagram b) Bode and Bode- phase diagram of the specimens with rough surface with maximum corrosion inhibitor concentration in 0.5 M H<sub>2</sub>SO<sub>4</sub> solution during immersion.

Figure 6a presents the nyquist diagram of the rough specimens in solution with 0.01 M BTA after 96h immersion. Since the highest corrosion resistance is for the rough specimen at the 0.01 M BTA concentration, the results of this specimen were reported at different times every 24 hours until 96 hours (see Table 3).

**Table 3.** parameters obtained by impedance data fitted by equivalent circuit and different levels of corrosion inhibitor efficiency in 0.5 M H<sub>2</sub>SO<sub>4</sub> solution in the presence of various concentrations of corrosion inhibitors in 96 h for mild steel.

BTA concentration (M)	Time (h)	R <sub>s</sub> (Ωcm <sup>2</sup> )	CPE <sub>1</sub> × 10 <sup>-4</sup> (mΩ <sup>-1</sup> cm <sup>-2</sup> s <sup>n</sup> )	n <sub>1</sub>	R <sub>1</sub> (Ωcm <sup>2</sup> )	%IE
Rough surface						
No BTA	0	2.9	7.2	0.65	22	-
	24h	2	9.8	0.85	12	-
	48h	2.3	9.5	0.82	13.1	-
	72h	2.8	8.0	0.83	14	-
	96h	2.7	6.5	0.85	15	-
0.0025M BTA	0h	3	4.6	0.65	49	55
	24h	3.5	5.0	0.75	50	76
	48h	4	7.0	0.75	37	64
	72h	3	6.2	0.77	35	60
	96h	3.7	5.5	0.77	34	56
0.005M BTA	0h	3.3	1.20	0.65	72	69
	24h	4	1.00	0.72	71	83
	48h	5	2.50	0.73	70	81
	72h	3	3.00	0.75	70	80
	96h	3.5	3.10	0.75	70	78
0.0075M BTA	0h	3.6	9.80	0.64	143	84
	24h	4.6	1.80	0.66	143	91
	48h	4.8	6.30	0.66	179	92
	72h	10	1.60	0.68	199	93
	96h	17.4	2.00	0.68	195	92
0.01M BTA	0h	7	9.80	0.65	143	84
	24h	5	1.00	0.72	151	92
	48h	6	0.5	0.72	162	92
	72h	10	0.7	0.73	170	92
	96h	16	0.7	0.73	175	91
Smooth surface						
No BTA	0h	6.6	3.1	0.91	22	-
	24h	6	1.5	0.7	17	-
	48h	6	1.4	0.7	19	-

	72h	7	3.1	0.75	23	-
	96h	6.5	2.1	0.72	23	-
0.0025M BTA	0h	3.3	2.8	0.89	56	61
	24h	3.3	3.2	0.8	52	67
	48h	3.9	4.0	0.78	45	58
	72h	3.1	3.8	0.78	37	38
	96h	3	3.3	0.77	32	28
0.005M BTA	0h	6.5	5.0	0.91	86	74
	24h	7	1.0	0.86	85	80
	48h	7	0.5	0.86	89	79
	72h	7	0.9	0.84	75	69
	96h	6.5	1	0.84	73	68
0.0075M BTA	0h	2.5	3.2	0.9	139	84
	24h	2.9	1.0	0.87	142	88
	48h	3.5	0.5	0.87	140	86
	72h	2.5	0.5	0.85	140	83
	96h	3	1.0	0.85	139	83
0.01M BTA	0h	3	1.8	0.91	148	85
	24h	3.2	1.0	0.9	155	89
	48h	3.6	0.5	0.88	163	88
	72h	3.5	0.2	0.87	175	87
	96h	3.9	0.4	0.87	170	86

As figure 6 suggests, by increasing the time, the semicircle radius is fixed until a day and after that it increased. This result indicates that by increasing the corrosion inhibitor concentration, the quality of the protective layer is improved. Selvi et al. [1] showed that by increasing the exposure time, the thickness and quality of oxide layer is improved and this increases resistance but they have considered chemisorption with the formation of oxide layer while the initial results of potentiodynamic polarization test indicate physisorption. Nyquist curve results showed increasing in resistance after two days of immersion. The pitting corrosion is seen over the time and this was observed by the changes in the final points of bode-phase curve (see in Figure 6b). The equivalent circuit is also presented based on an inductor that indicates pitting and this equivalent diagram is shown in Figure 7. These changes and more accurate analysis are presented in section 3-6.

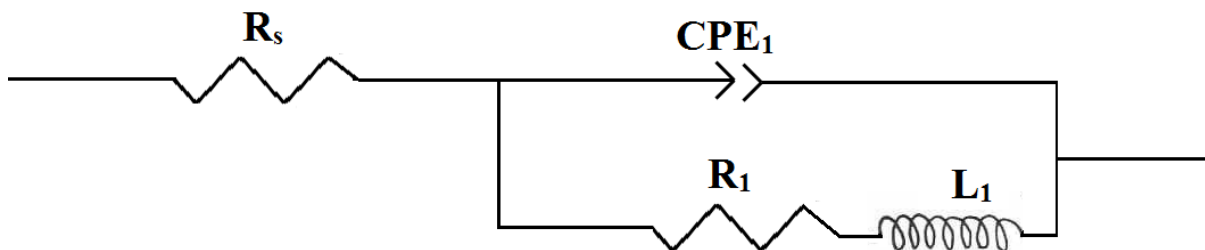


**Figure 7.** Equivalent circuit to fit the impedance curves for rough specimens immersed in 0.5 M  $H_2SO_4$  solution in the presence of 0.01 M BTA after the second day.

To investigate the effect of immersion time, bode and bode-phase curves are plotted in Figure 6. The curves showed single time constant and indicated that there is only one barrier layer against water and aggressive ions. Since the second day, changes in the lower frequency parts of the diagrams were observed and as discussed earlier, they are associated with pitting and the inductor element in the equivalent electrical circuit. As it can be observed, since the second day and by increasing resistance, the phase angle is reduced insignificantly which indicates a change in resistance against the aggressive ions. Bode curve indicates the increased resistance over time at the frequency of 0.01 Hz. It is notable in bode curves that the solution resistance is higher at 72 h and 96 h than the rest of immersion times which is a reason to change in mechanism and it indicates that at these times, the soluble ions have hardly reached the interface between the substrate and solution. As it was mentioned earlier, it could have happened by a change in mechanism.

Table 3 presents the parameters obtained for the fitted impedance data with the equivalent circuit and corrosion inhibitor efficiency for mild steel. Analysis of the changes in resistance, capacitance and  $n$  also are reported in table 3. It is clear, over immersion time, the resistances of both smooth and rough surfaces are reduced in the absence of corrosion inhibitor and this reduction is higher for the rough specimen. In the absence of the corrosion inhibitor, the surface is not protected and since the porous products of corrosion reaction, have no protective ability. So, the resistance is reduced over time and this reduction is higher in the case of rough specimen due to the increase in the active areas and corrosion exacerbation. In other specimens, no other particular behavior is observed by increasing immersion time and concentration of BTA. According to table 3, the values of  $n_1$  for the smooth specimen are between 0.7 and 0.9, and it is between 0.65 and 0.85 for the rough specimen. It could be associated with the inevitable reduction in heterogeneity of the initial surface as the result of adsorbing the corrosion inhibitor on the active sites. The reported results of  $n$  are a criterion of surface roughness that is consistent with the results of the measured roughness value.

Table 3 presents capacitance changes by immersion time and with increasing in corrosion inhibitor concentration. By increasing the concentration of corrosion inhibitor, the numerical values of  $CPE_1$  (fitness factor) are reduced which indicates that the BTA molecules delay the passage of ions by being adsorbed on the steel solution interface and prevent the arrival of ions to the substrate.

Corrosion inhibitor efficiency percentage is obtained by charge transfer resistance obtained from the nyquist curve, using the following equation:

$$IE_2\% = (1 - R_1^0/R_1) \times 100 \quad (8)$$

Where,  $R_1$  and  $R_1^0$  are charge transfer resistance with and without corrosion inhibitor, respectively [45]. Corrosion inhibitor efficiency is presented in Table 3 and it is obvious that this value is increased by increasing corrosion inhibitor concentration. At the concentration of 0.01 M of corrosion inhibitor it reached the maximum value of 92% for the rough specimen. It can be concluded that the corrosion inhibition efficiency calculated by weight loss, potentiodynamic polarization and EIS have appropriate match.

### 3.5. Examining the effects of other types of roughness on corrosion

It is clear that the highest corrosion inhibition is obtained in the presence of 0.01 M BTA for rough surface but the surface roughness, as previously discussed has a direct impact on the adsorption of the corrosion inhibitor molecules. To investigate the effect of roughness on the corrosion resistance of steel specimens in 0.5 M  $H_2SO_4$  solution with and without 0.01 M BTA, the potentiodynamic polarization tests were conducted on the surfaces prepared by sandpapers with grade numbers of #60, #120, #320, #800, #1500 and #3000. The resultant efficiency is presented in Fig. 8.

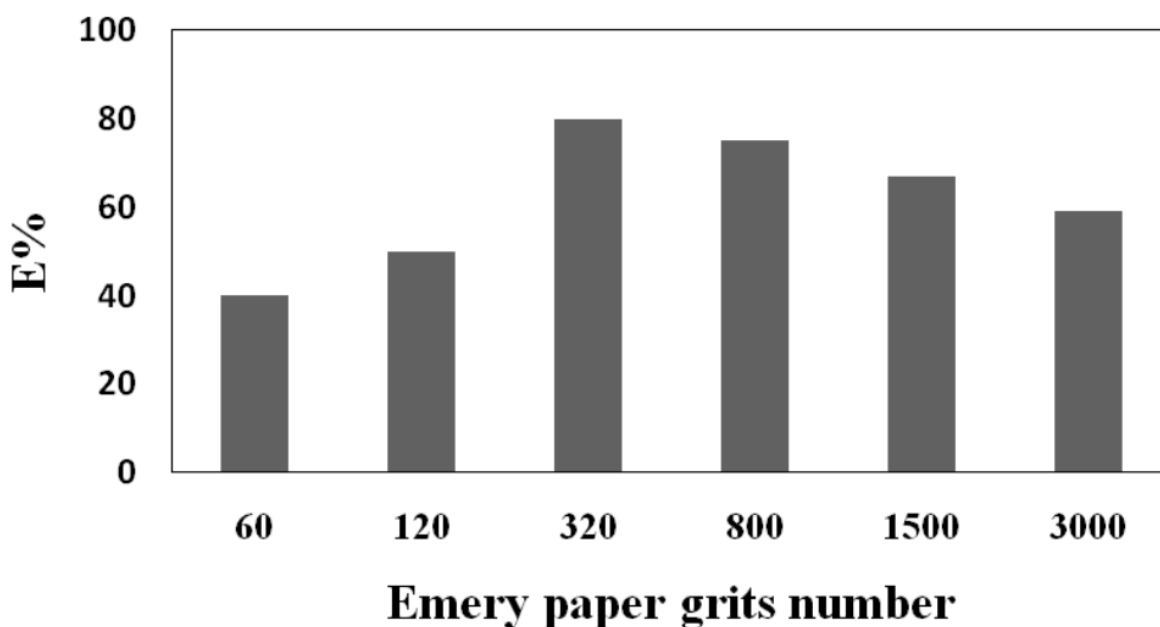


**Figure 8.** Changes in inhibition efficiency in terms of sandpaper grade number.

As it is clear, by increasing surface roughness, the curve moves towards lower values, which indicates reduction of corrosion resistance. The reason is probably the increasing of corrosion acceleration factors such as deeper cavities on the surface of specimen. Also the concentration of the corrosion inhibitor is not capable of protecting these surfaces because by increasing roughness, the real surface in contact with the electrolyte will increase. Also by reducing roughness, the corrosion inhibition percentage is reduced as discussed earlier, due to the low adsorbed molecules [46].

## 3.6. Mechanism study

By analyzing the impedance curves at the beginning of immersion and potentiodynamic polarization curves, it is clear that the initial mechanism has been through the adsorption of BTA molecules and corrosion inhibition is done by forming a layer of BTA. As it was mentioned earlier, the rough sample in solution with 0.01 M BTA has also presented higher resistance both in the EIS and potentiodynamic polarization. Surface roughening, on one hand, increased actual surface and this increase, leads to the higher number of BTA molecules on the surface and more surface protection [44], and on other hand, caused the surface to have stronger Van der Waals bonds with the corrosion inhibitor molecules, due to the changes in bonding energies. It can be said that roughening increased the tendency to form a bond with corrosion inhibitor molecules [43]. The increase in the actual surface and its effect on the number of adsorbed molecules as described in section 3.3, is discussed by the surface coverage to growing factor of surface parameters ratio. The increase in this ratio from 0.46 to 0.53, is a reason for the increase in number of corrosion inhibition molecules which adsorbed on the surface. By passing immersion time, the impedance curves are changed and an inductive loop was added to them. They were fitted with an inductor on the third and fourth day of immersion which indicates surface layer was destroyed.

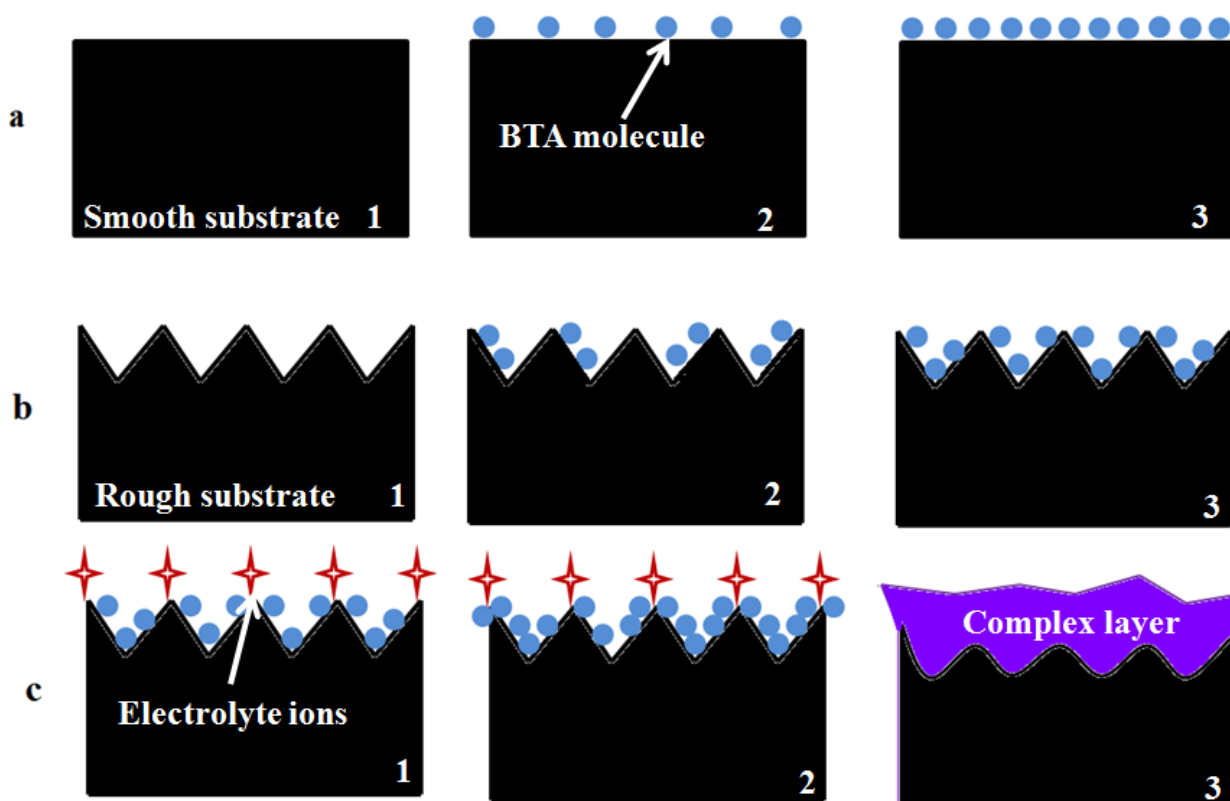


**Figure 9.** The schematic image of adsorbing inhibiting molecules on the a) smooth, b) rough and c) rough surfaces over time.

As reported in [47], if the corrosion inhibitor concentration on the surface is higher than the critical level, its film formation mechanism is converted to the complex formation and as reported in

[1], by passing immersion time, the resistance of the specimen is increased which is due to the thickening of the oxide layer. However, probably by passing immersion time, due to changes in surface conditions, penetration of aggressive ions and damage of the adsorption layer was increased. After the third day, more adsorption of the BTA and the formation of corrosion products and their possible interaction will change the corrosion inhibition mechanism. Its dominant mechanism is the formation of the complex layer and protective abilities of this layer becomes higher by passing the time.

The reason that this complex layer is more formed on the rough surface, is that the concentration of adsorbed corrosion inhibitor on the surface is an important factor on the complex layer's quality [48]. In the case of rough specimen, the adsorption of corrosion inhibitor molecules was higher due to the mentioned reasons. It is natural that the complex layer formed on the rough sample has better quality and higher protective effect.

To better understand the discussed mechanism, the schematic figure is presented in Figure 9. Figure 9a and 9b indicate that by roughening, or increasing the real surface, more corrosion inhibitor molecules are adsorbed on the surface. When the BTA concentration reaches a critical value, by presence of corrosion inhibitor molecules, more protection was done. Figure 9c shows the changes of mechanism over the immersion time. By passing of time, surface will change and a complex layer will form. The formed complex layer, at the presence of the corrosion inhibitor molecules and the corrosion products are shown in Figure 9c [47].

## 4. SURFACE ANALYSIS

### 4.1. SEM analysis

The SEM images of the raw specimens, specimens immersed in acidic solution and specimens immersed in inhibited acidic solution are presented in Figure 10. As it can be seen from this figure, the steel surface is destroyed in the absence of corrosion inhibitor more than the presence of BTA. To present the sanding lines more clearly in Fig. 10a, the SEM image with higher magnification is presented in the top right corner of this image. For both specimens (Figs. 10a,b), more damage can be seen in the absence of corrosion inhibitor. It can be seen that before immersion, the surface of the steel specimens are smooth (Fig. 10b). It seems that when the surface of the specimen immersed in a solution without corrosion inhibitor, it will severely corroded (Fig. 10d), and the layer of corrosion products can be seen.

Thus the porous surfaces are obtained, however less damage is caused in the presence of corrosion inhibitor on the surface [49]. The results obtained from measuring the roughness with the surface profilometer due to roughness profiles are presented in Figure 11. The  $R_a$  parameter for the smooth specimen before immersion is  $0.12 \pm 0.01 \mu\text{m}$  and this parameter was increased after immersion in the solution with corrosion inhibitor and reached the value of  $2.56 \pm 0.01 \mu\text{m}$ .  $R_a$  for the smooth specimen which immersed in the solution without corrosion inhibitor reached to  $2.96 \pm 0.01 \mu\text{m}$ . Increase of  $R_a$  for the smooth specimen was also reported elsewhere [50], for the immersion of

polished specimens immersed in 1 M HCl solution with and without Turmeric extract (TE) as corrosion inhibitor. In the solution containing corrosion inhibitor,  $R_a$  presented less increase which is associated with the corrosion inhibition ability and film formation of the metal's surface [51].  $R_a$  was  $4.39 \pm 0.01 \mu\text{m}$  for the rough specimen before immersion.

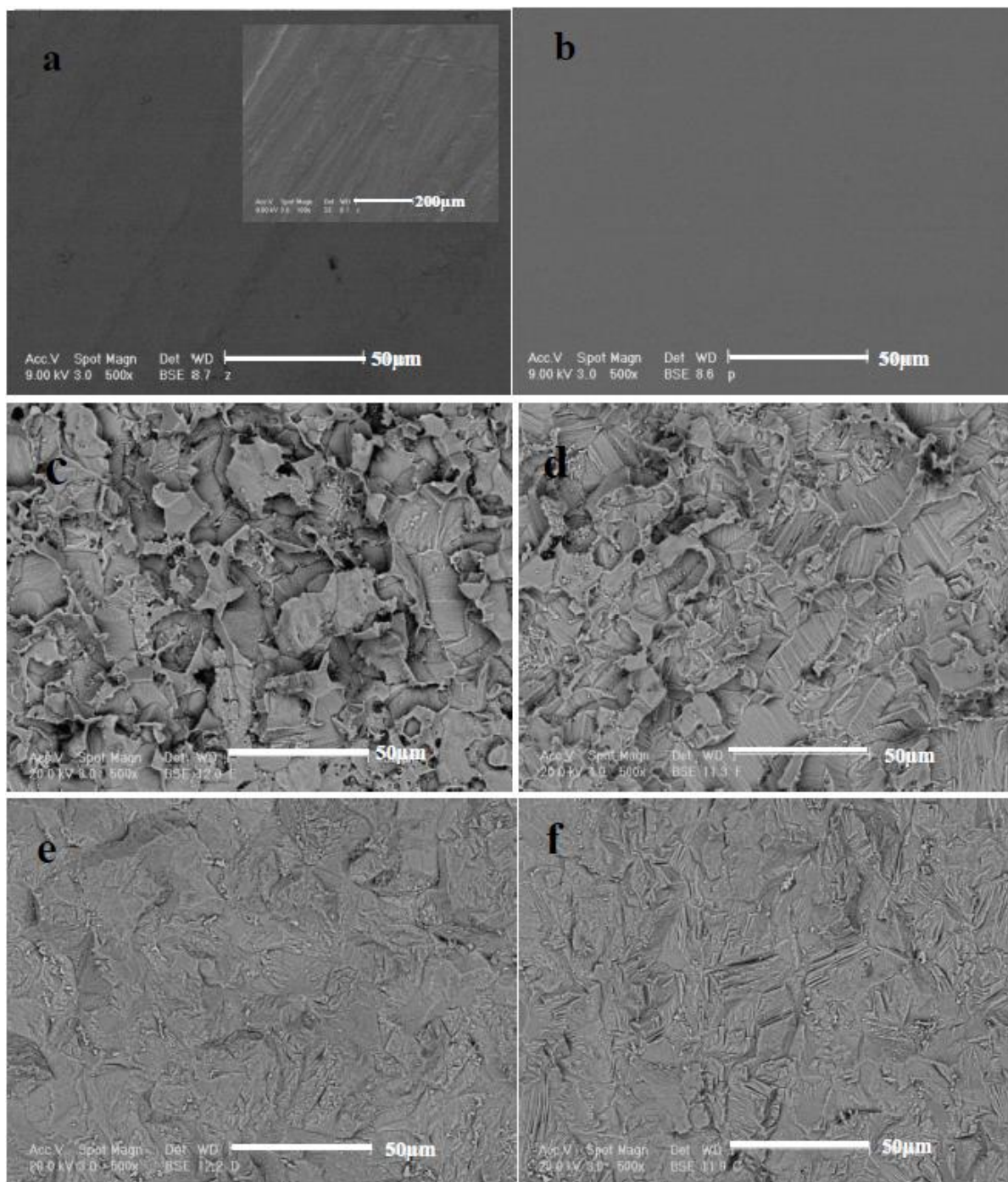


**Figure 10.** SEM image a) steel with a rough surface b) steel with a smooth surface c) rough steel after immersion in a solution without corrosion inhibitor d) smooth steel after immersion in a solution without corrosion inhibitor e) rough steel after immersion in a solution with corrosion inhibitor f) smooth steel after immersion in a solution with corrosion inhibitor.

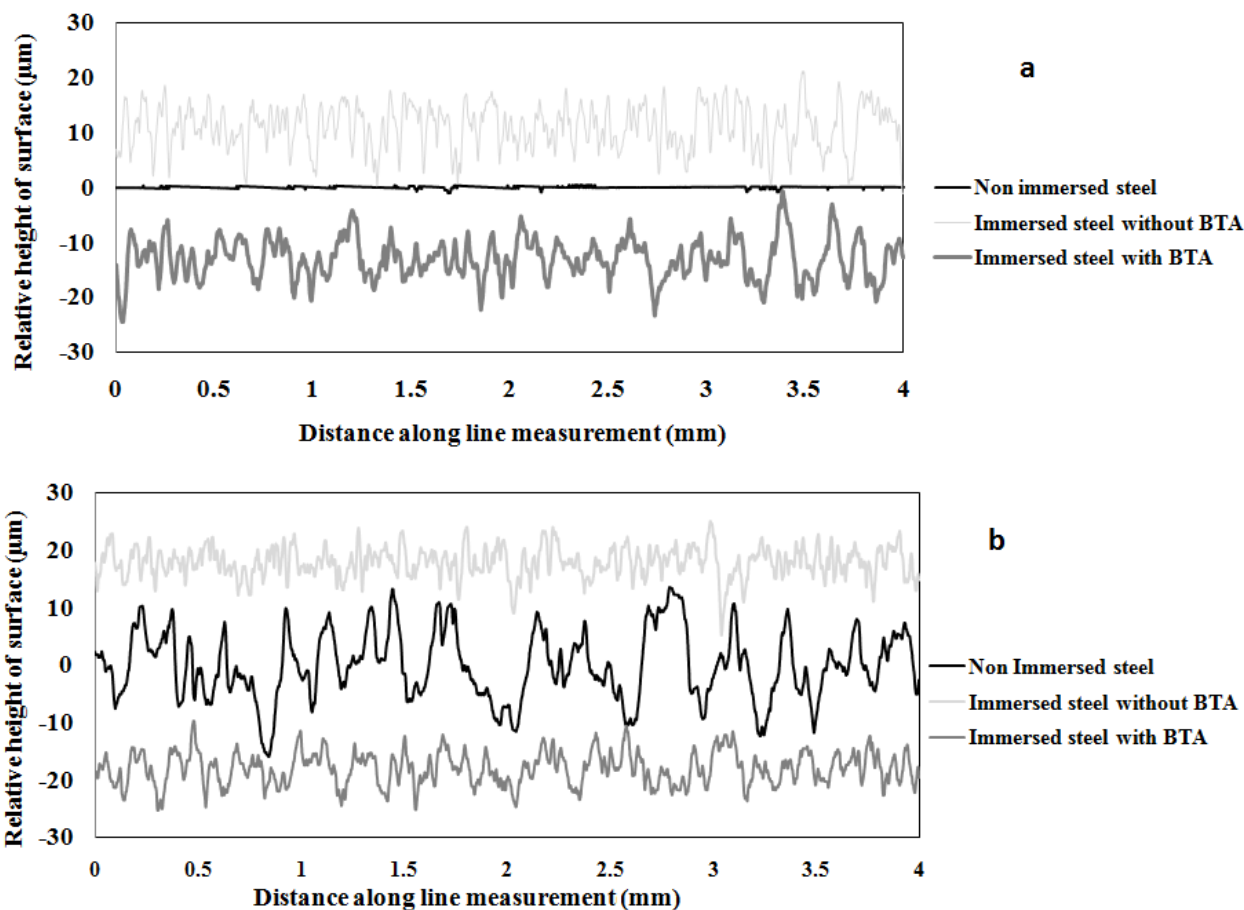


**Figure 11.** The roughness profile of the steel specimen with a) smooth and b) rough surfaces before and after immersion in 0.5 M H<sub>2</sub>SO<sub>4</sub> solution with and without corrosion inhibitor.

It was reduced to  $1.92 \pm 0.01 \mu\text{m}$  in a solution without corrosion inhibitor while in the solution containing corrosion inhibitor; the roughness has less reduction and reached  $2.35 \pm 0.01 \mu\text{m}$ . The  $R_a$  for rough specimen is reduced after immersion due to the corrosion but this parameter showed less reduction when the specimens immersed in solution with corrosion inhibitor. The reduction in this parameter is observed after immersion, which indicates that the peak is preferably dissolved and smoother surface is provided [7, 51]. Lower reduction of  $R_a$  in the solution with corrosion inhibitor, in the case of rough specimen could be associated with ability of corrosion inhibitor film formation on the steel surface.

$R_{10}$  parameter is a ratio between the measured length along the profile curve and profile length which was presented in percentage and its values are usually between 0 and 10% [52]. The length of the scanned profile for roughness measurement by surface profilometer is 4mm and the  $R_{10}$  parameter value for the specimen abraded up to #320 is 3.28% and for the specimen polished up to #3000 is 0.156%. Thus the actual lengths of the profile for the rough and smooth specimens are 4.1312 and 4.0056 mm. In section 3.3, using the equation 4, the surface coverage parameter after the potentiodynamic polarization test in 0.5 M H<sub>2</sub>SO<sub>4</sub> solution containing 0.01 M BTA is 0.8 and 0.59 for the rough and smooth specimens, respectively. By dividing the surface coverage number to the actual length, the values of 0.193 and 0.147 are obtained for rough and smooth specimens (see Table 4). It

could confirm the proposed mechanism in section 3.5, because the higher values of this ratio for the rough specimen reflects the fact that in addition that the rough surface has higher real surface area, the ratio of corrosion inhibitor molecules to the real surface, is higher for rough surface.

**Table 4.**  $R_{10}$  parameters for the rough and smooth specimens before immersion in solution,  $\Theta$  obtained from the potentiodynamic polarization test which includes optimal corrosion inhibitor concentration, the actual length of profile and the ratio between  $\Theta$  and the actual length of profile for the rough and smooth specimens

	$R_{10}$	Actual length(mm)	$\Theta$	/actual length $\Theta$
Rough surface	3.28%	4.1321	0.8	0.193
Smooth surface	0.156%	4.0056	0.59	0.147

**Table 5.**  $R_{10}$  and  $R_a$  parameters for the rough and smooth specimens before and after immersion in 0.5 M  $H_2SO_4$  solution including 0.01 M BTA and without BTA

	$R_a(\mu\text{m})$	$R_{10}(\%)$
Rough surface		
non immersed steel	4.39	3.28
immersed steel without BTA	1.92	5.07
immersed steel with BTA	2.35	3.01
Smooth surface		
non immersed steel	0.121	0.156
immersed steel without BTA	2.96	8.6
immersed steel with BTA	2.56	3.02

After immersion, the  $R_{10}$  parameter changed similar to  $R_a$  from the values of 0.156% and 3.28% before immersion to the values of 8.6% and 5.07% after immersion in the solution without BTA for the rough and smooth specimens, respectively. Also it reaches 3.02% and 3.01% in solution containing BTA. This number increased for the smooth specimen such as the  $R_a$ , and this increase is more significant in the solution without corrosion inhibitor. It also reduced for the rough specimen in the solution with corrosion inhibitor but in the case of solution without corrosion inhibitor, it increased despite the reduction in  $R_a$ . Changes in both parameters are presented in Table 5 for both samples based on the type of immersion solution.

## 4.2. Fourier-transform infrared Spectroscopy (FT-IR)

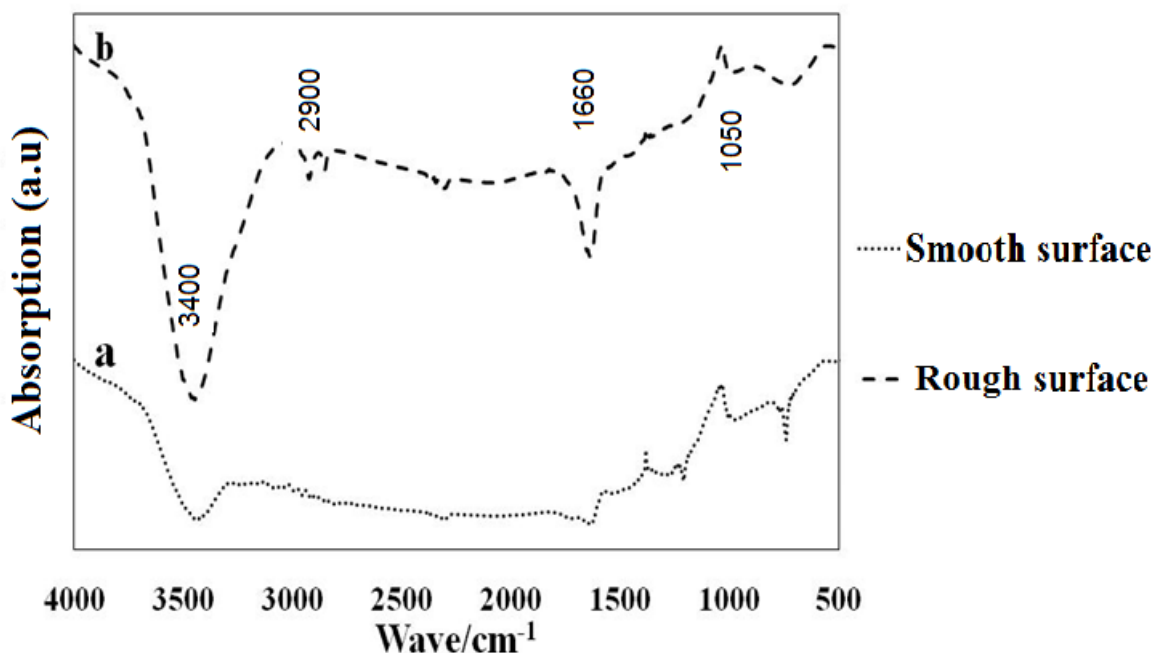


**Figure 12.** a) the FTIR spectrum for the scraped material from the surface of steel with smooth surface  
 b) the FTIR spectrum for the scraped material from the surface of steel with rough surface immersed in 0.5 M H<sub>2</sub>SO<sub>4</sub> solution with 0.01 M BTA

FTIR spectrum is very strong to determine and predict the types of bonds between the organic active agents adsorbed on the surface of solids. Figure 12 presents FTIR spectrum for the scraped material from the surface of rough specimen after immersion in 0.5 M H<sub>2</sub>SO<sub>4</sub> solution with 0.01 M BTA. This spectrum is obtained between 500 and 4000 cm<sup>-1</sup>. In case of BTA, the stretching bond N-H presents a strong peak around 3400 cm<sup>-1</sup> and the stretching bond C-H presents a weak peak in the range of 2900-3100 cm<sup>-1</sup> and the N-H bonds are presented in the range 1500-1600 cm<sup>-1</sup>. The vibrating stretching bond C-N presents a strong peak within the range of 1300-1450 cm<sup>-1</sup> [1, 53].

There is a broad peak around 3500 cm<sup>-1</sup> and this peak is associated with the O-H stretching bond with water. The peak around 1600 cm<sup>-1</sup>, was observed for both surfaces and as mentioned earlier, it is associated with N-H bond. Within 2900 cm<sup>-1</sup>, a weak peak is observed which is more evident for the rough specimen. This peak is associated with the aromatic C-H stretching bond. This peak is a proof of the presence of BTA on the steel's surface and due to the stronger peak for rough specimen; BTA has been more adsorbed on this surface. The next peak is around 1660 cm<sup>-1</sup> which is associated with the vibration bending bond OH<sub>2</sub> and the next peak in the range of 1000 cm<sup>-1</sup> which is due to vibrating bond O-Fe-O.

## 5. CONCLUSION

The corrosion inhibition effect of BTA in 0.5 M H<sub>2</sub>SO<sub>4</sub> solution has shown that by increasing the corrosion inhibitor concentration, the corrosion inhibitor efficiency is increased and for the smooth

specimen in the presence of 0.01M BTA, it reaches 59%. In the case of rough specimen with  $R_a=4.3$   $\mu\text{m}$ , it showed a devastating effect on corrosion of steel in the solution without corrosion inhibitor. It increased the corrosion current density; while surface roughening causes much decrease in the corrosion rate in the solution containing corrosion inhibitor compared to the smooth specimen and has led to the corrosion inhibition efficiency of 80% in the presence of 0.01 M BTA. Immersion in 0.5 M  $\text{H}_2\text{SO}_4$  solution, for the rough specimens, reduced the  $R_a$  roughness parameter in the absence of corrosion inhibitor. Thus, this decrease in roughness was more in the solution without corrosion inhibitor. The opposite was occurred for the polished specimen and its roughness was increased by corrosion in the solution without corrosion inhibitor. Analyzing the adsorption isotherm at 25 °C showed that the adsorption energy increased for rough specimen in comparison with smooth specimen. The higher adsorption energy for the rough specimen indicates the stronger adsorption of the corrosion inhibitor on the surface of the rough specimen. The value of the released energy indicates greater tendency to physisorption of the corrosion inhibitor. The adsorption in both surfaces followed the langmuir isotherm.

## References

1. S.T. Selvi, V. Raman, N. Rajendran, *J Appl Electrochem*, 33 (2003) 1175-1182.
2. S.A. El-Rehim, M.A. Ibrahim, K. Khaled, *J Appl Electrochem*, 29 (1999) 593-599.
3. G. Schmitt, *British Corrosion Journal*, (2013).
4. P. Chatterjee, M. Banerjee, K. Mukherjee, *Indian J Technol*, 29 (1991) 191-194.
5. S.A. El Rehim, M.A. Ibrahim, K. Khalid, *Mater Chem Phys*, 70 (2001) 268-273.
6. M. Mennucci, E. Banczek, P. Rodrigues, I. Costa, *Cement Concrete Comp*, 31 (2009) 418-424.
7. E. Barmatov, T. Hughes, M. Nagl, *NACE Int*, (2014).
8. S. Ghareba, S. Kwan, S. Omanovic, *J Electroche Sci Eng*, 5 (2015) 157-172.
9. G.K. Gomma, *Mater Chem Phys*, 55 (1998) 235-240.
10. J. Aljourani, K. Raeissi, M. Golozar, *Corr Sci*, 51 (2009) 1836-1843.
11. A. Popova, *Corr Sci*, 49 (2007) 2144-2158.
12. Y. Feng, Y.F. Cheng, *J Mater Eng Perform*, 24 (2015) 4997-5001.
13. E. Naderi, A. Jafari, M. Ehteshamzadeh, M. Hosseini, *Mater Chem Phys*, 115 (2009) 852-858.
14. W. Li, D. Li, *Acta Mater*, 54 (2006) 445-452.
15. W. Deng, P. Lin, Q. Li, G. Mo, *Corr Sci*, 74 (2013) 44-49.
16. A. Standard, *Am Socr Test Mater G1-03*, (2004).
17. A.S.f. Testing, Materials, in ASTM G31-72: Standard Practice for Laboratory Immersion Corrosion Testing of Metals, ASTM, (2004).
18. X. Li, S. Deng, H. Fu, T. Li, *Electrochim Acta*, 54 (2009) 4089-4098.
19. A. Designation, in Standard Reference Test Method for Making Potentiostatic and Potentiodynamic Anodic Polarization Measurements, ASTM Int Conshohocken, Pa, USA, (1999).
20. A. G106-89, (2010).
21. G. Avci, *Colloids and Surfaces A: Physicchem Eng*, 317 (2008) 730-736.
22. R. Solmaz, G. Kardaş, B. Yazıcı, M. Erbil, *Colloids Surf A: Physicoche Eng*, 312 (2008) 7-17.
23. A. Arancibia, J. Henriquez-Roman, M. Paez, L. Padilla-Campos, J. Zagal, J. Costamagna, G. Cárdenas-Jirón, *J Solid State Electr*, 10 (2006) 894-904.
24. S. Omanovic, S. Roscoe, *Corr*, 56 (2000) 684-693.
25. K. Boumhara, M. Tabyaoui, C. Jama, F. Bentiss, *J Ind Engineering Chem*, 29 (2015) 146-155.
26. S.K. Shukla, M. Quraishi, E.E. Ebenso, *Int. J. Electrochem. Sci*, 6 (2011) 2912-2931.

27. F.M. Donahue, K. Nobe, *J Electrochem Soc*, 112 (1965) 886-891.
28. O.K. Abiola, Y. Tobun, *Chinese Chem Lett*, 21 (2010) 1449-1452.
29. M. Morad, A.K. El-Dean, *Corr Sci*, 48 (2006) 3398-3412.
30. M. Lebrini, M. Traisnel, M. Lagrenée, B. Mernari, F. Bentiss, *Corr Sci*, 50 (2008) 473-479.
31. G. Moretti, F. Guidi, G. Grion, *Corr sci*, 46 (2004) 387-403.
32. N. Hackerman, E. Snavely, J. Payne, *J Electrochem Soc*, 113 (1966) 677-681.
33. T. Murakawa, S. Nagaura, N. Hackerman, *Corr Sci*, 7 (1967) 79-89.
34. E. Blomgren, J. Bockris, *J Phys Chem*, 63 (1959) 1475-1484.
35. B. El Mehdi, B. Mernari, M. Traisnel, F. Bentiss, M. Lagrenee, *Mater chem and phys*, 77 (2003) 489-496.
36. J. Uehara, K. Aramaki, *J Electrochem Soc*, 138 (1991) 3245-3251.
37. J.R. Macdonald, *Ann Biomed Eng*, 20 (1992) 289-305.
38. K.M. Ismail, A.A. El-Moneim, W.A. Badawy, *J Electrochem Soc*, 148 (2001) C81-C87.
39. G. Brug, A. Van Den Eeden, M. Sluyters-Rehbach, J. Sluyters, *J Electroanal Chem*, 176 (1984) 275-295.
40. J.-B. Jorcin, M.E. Orazem, N. Pébère, B. Tribollet, *Electrochimic Acta*, 51 (2006) 1473-1479.
41. M.-C. Zhao, M. Liu, G.-L. Song, A. Atrens, *Corr Sci*, 50 (2008) 3168-3178.
42. K.V. Kumar, M.S.N. Pillai, G.R. Thusnavis, *J Mater Sci Technol*, 27 (2011) 1143-1149.
43. E.A. Noor, *MaterChem Phys*, 131 (2011) 160-169.
44. R.B. Alvarez, H.J. Martin, M. Horstemeyer, M.Q. Chandler, N. Williams, P.T. Wang, A. Ruiz, *Corr Sci*, 52 (2010) 1635-1648.
45. K. Khaled, *Electrochimic Acta*, 54 (2009) 4345-4352.
46. A.K. Singh, P. Singh, *J Ind Eng Chem*, 21 (2015) 552-560.
47. G. Lewis, *Corr*, 34 (1978) 424-428.
48. A. Popova, E. Sokolova, S. Raicheva, M. Christov, *Corr Sci*, 45 (2003) 33-58.
49. K. Krishnaveni, J. Ravichandran, *J Electroanal Chem*, 735 (2014) 24-31.
50. M. Nasibi, M. Mohammady, A. Ashrafi, A.A.D. Khalaji, M. Moshrefifar, E. Rafiee, *J Adhes Sci Technol*, 28 (2014) 2001-2015.
51. B. Evgeny, T. Hughes, D. Eskin, *Corr Sci*, 103 (2016) 196-205.
52. W. Kabsch, *Acta Crystallogr Section D: Biological Crystallography*, 66 (2010) 125-132.
53. Y. Ling, Y. Guan, K. Han, *Corr*, 51 (1995) 367-375.